arXiv:cond-mat/0609494v4 [cond-mat.stat-mech] 28 May 2007

Violation of the fluctuation-dissipation theorem in a protein system

Kumiko Hayashi and Mitsunori Takano
Department of Physics, Waseda University, Tokyo 169-8555, Japan
(Dated: February 6, 2008)

We report the results of molecular dynamics simulations of the protein myosin carried out with an elastic network model. Quenching the system, we observe glassy behavior of a density correlation function and a density response function that are often investigated in structure glasses and spin glasses. In the equilibrium, the fluctuation-response relation, a representative relation of the fluctuation-dissipation theorem, holds that the ratio of the density correlation function to the density response function is equal to the temperature of the environment. We show that in the quenched system that we study, this relation can be violated. In the case that this relation does not hold, this ratio can be regarded as an effective temperature. We find that this effective temperature of myosin is higher than the temperature of the environment. We discuss the relation between this effective temperature and energy transduction that occurs after ATP hydrolysis in the myosin molecule.

PACS numbers: 87.14.Ee, 05.70.Ln, 05.40.-a

I. INTRODUCTION

Proteins possess complex structures and, consequently, complex motion. Such complexity might be necessary to carry out the functions exhibited by living organisms. Statistical properties of the types of complex structure and motion characterizing protein molecules have been studied using various approaches, in particular, that employing energy landscapes [1]. Recently, with a computation of the density of states for a Gō-like model of a protein, statistical properties were investigated using the idea of inherent structures [2]. An inherent structure is a subset of the configuration space that represents the local minima of an energy landscape, originally proposed to study the dynamics of liquids [3]. Although the idea of inherent structures is very important to understand protein dynamics, it is difficult to directly experimentally investigate the inherent structures of a protein. For this reason, it would be useful if we could characterize the energy landscape of a protein in forms of experimentally measurable quantities, such as a density correlation function or a density response function.

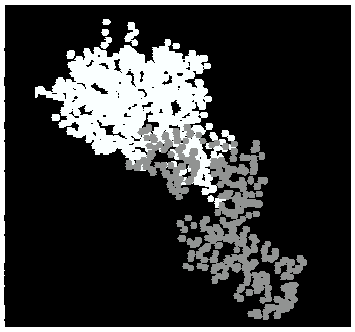

FIG. 1: Schematic depiction of the myosin molecule (1KK7 [17]). The horizontal axis denotes the x direction, and the vertical axis denotes the y direction. According to our convention, the α-carbon atoms, C_α with with $i = 1, \cdots, 770$ belong to the head substructure (white), and those with $i = 771, \cdots, 1101$ belong to the tail substructure (gray). See the next section for the way how to number C_α atoms.

In structure glasses, which, like protein molecules, also possess energy landscapes with many local minima, statistical properties are often studied by computing the density correlation function and the density response function [4, 5, 6, 7, 8, 9]. In equilibrium, these quantities satisfy the fluctuation-response relation, a representative relation in the fluctuation-dissipation theorem [10]. This relation means the equality of the ratio of the density correlation function to the density response function and the temperature of the environment [10]. For glassy systems, which exhibit slow relaxation and are inherently non-equilibrium, it has been reported that the fluctuation-response relation is violated [4, 5, 6, 7, 8, 9]; that is, the ratio of the relevant density correlation function and density response function is not equal to the temperature of the environment. The slow relaxation displayed by a glassy system, which results from the nature of its energy landscape, with many local minima, can be characterized by a quantity representing the degree of violation of the fluctuation-response relation. In some cases that the fluctuation-response relation is violated, the ratio of the density correlation function to the density response function has interpreted as an "effective temperature," and there are studies addressing the question of whether this effective temperature can play the role of the temperature in non-equilibrium systems [4, 5, 6, 7, 8, 9].

In this paper, we report the results of simulations of molecular dynamics employing an elastic network model of sub-fragment 1 of a myosin molecule, which is composed of a head substructure, with ATP-binding and actin-interacting sites, and a tail substructure, with a long alpha-helix bound by two light chains (see Fig. 1). With the hypothesis that appropriate density correlation function and density response function, which have not yet been fully exploited in studies of protein dynamics, can be used to characterize the glassy behavior of pro-

tein molecules, we compute such quantities in the case of a quenched system. While elastic network models have been used to study the elastic properties of equilibrium fluctuations [11, 12], such models have not been used to study non-equilibrium behavior. In this paper, we show that glassy, non-equilibrium behavior can also be described with this class of models.

Because the effective temperature that we employ represents the degree to which the behavior of the system is "glassy," we quantitatively investigate the complexity of the myosin's head through use of this effective temperature. More specifically, we compute the values of the effective temperature for both the head and the tail, and we compare these values with the temperature of the environment. We also seek to elucidate the origin of the observed glassy behavior through analysis that investigates the inherent structures [3]. We find that the inherent structure for the model we study has a resemblance to the structure of a structural isomer of myosin determined by X-ray crystallography.

II. ELASTIC NETWORK MODEL

In our study, a protein molecule is regarded as consisting of α-carbon atoms, C_α, employing a coarse-grained representation of amino acid residues [13, 14, 15]. A C_α atom is a constituent of the carbon skeleton of a protein molecule.

The position and velocity of the i-th C_α in a myosin molecule are denoted by $\boldsymbol{r}_i = (x_i, y_i, z_i)$ and $\boldsymbol{v}_i = (v_{xi}, v_{yi}, v_{zi})$, where $i = 1, \cdots, N$, and N is the total number of C_α atoms in the myosin molecule. Here, C_α atoms are numbered in the order of the heavy chain, the essential light chain and the regulatory light chain.

The Hamiltonian of our model is given by

$$H(\{\boldsymbol{r}_i\},\{\boldsymbol{v}_i\}) = \sum_{i=1}^{N} \frac{m}{2}|\boldsymbol{v}_i|^2 + V(\{\boldsymbol{r}_i\}) + V_{\rm trap}(\{\boldsymbol{r}_i\}), \quad (1)$$

where m is the mass of the i-th C_α, and $V(\{\boldsymbol{r}_i\})$ is the interaction potential

$$\begin{aligned} V(\{\boldsymbol{r}_i\}) &= \sum_{i}^{N-1} \frac{k_1}{2}(|\boldsymbol{r}_i - \boldsymbol{r}_{i+1}| - |\boldsymbol{r}_i^0 - \boldsymbol{r}_{i+1}^0|)^2 \\ &+ \sum_{i}^{N-1} \frac{k_2}{2}(|\boldsymbol{r}_i - \boldsymbol{r}_{i+2}| - |\boldsymbol{r}_i^0 - \boldsymbol{r}_{i+2}^0|)^2 \\ &+ \sum_{i}^{N-1}\sum_{j=i+3}^{N} \frac{k_3}{2}(|\boldsymbol{r}_i - \boldsymbol{r}_j| - |\boldsymbol{r}_i^0 - \boldsymbol{r}_j^0|)^2. \quad (2) \end{aligned}$$

We stipulate that $k_\ell = 0$ ($\ell = 1, 2, 3$) if $|\boldsymbol{r}_i^0 - \boldsymbol{r}_j^0| > r_{\rm c}$, where $r_{\rm c}$ is a cut-off length, and we set $k_2 = 0.5k_1$ and $k_3 = 0.1k_1$. With this form of $V(\{\boldsymbol{r}_i\})$, the configuration of the native structure, $\{\boldsymbol{r}_i^0\}$, is most stable. The values of the parameters $\boldsymbol{r}_i^0$ used here were taken from the RCSB Protein Data Bank [16]. Here, we chose the values of $\boldsymbol{r}_i^0$ so as to obtain the structure of the myosin molecule 1KK7 [17]. Also, these values are such that the center of mass is at $(0, 0, 0)$ and the unit of length is Å.

The function $V_{\rm trap}(\{\boldsymbol{r}_i\})$ that appears in (1) is a trapping potential that plays the role of an optical potential, acting to fix the molecule. This potential is given by

$$V_{\rm trap}(\{\boldsymbol{r}_i\}) = \sum_{i=350}^{400} \frac{1}{2}|\boldsymbol{r}_i - \boldsymbol{r}_i^0|^2 + \sum_{i=800}^{850} \frac{1}{2}|\boldsymbol{r}_i - \boldsymbol{r}_i^0|^2. \quad (3)$$

The time evolution of the system is described by the Langevin equation ($i = 1, \cdots, N$)

$$m\frac{{\rm d}\boldsymbol{v}_i}{{\rm d}t} = -\gamma\boldsymbol{v}_i - \frac{\partial H}{\partial \boldsymbol{r}_i} + \boldsymbol{\xi}_i(t), \quad (4)$$

$$\frac{{\rm d}\boldsymbol{r}_i}{{\rm d}t} = \boldsymbol{v}_i, \quad (5)$$

where $\boldsymbol{\xi}_i = (\xi_{xi}, \xi_{yi}, \xi_{zi})$ is Gaussian white noise that satisfies

$$\langle \xi_{\alpha i}(t)\xi_{\beta j}(t')\rangle = 2\gamma T\delta(t - t')\delta_{\alpha,\beta}\delta_{i,j}. \quad (6)$$

Here, T is the temperature of the environment (with the Boltzmann constant set to 1), and γ is the friction constant of the solvent. Here, $\langle\ \rangle$ denotes the average over all noise histories. We set the parameters used in our numerical simulations as $m = 1$, $\gamma = 0.01$, $k_1 = 1$, $N = 1101$ and $r_{\rm c} = 10$.

III. EQUILIBRIUM BEHAVIOR: FLUCTUATION-RESPONSE RELATION AT HIGH TEMPERATURE

In equilibrium, the ratio of the density correlation function to the density response function is equal to the temperature of the environment. This relation among the density correlation function, the density response function and the temperature of the environment is called the fluctuation-response relation (For a review of the fluctuation-dissipation theorem, including the fluctuation-response relation, see Ref. [10]).

In order to examine whether the fluctuation-response relation holds for our system, we first introduce a density response function. In this section, we consider the relaxation process that results in the case that the system is initially in equilibrium, and then at $t = 0$ the perturbing potential

$$\sum_{i=1}^{N} V_{\rm p}(y_i) \equiv \sum_{i=1}^{N} \Delta\cos(ky_i) \quad (7)$$

is added to the Hamiltonian (1). Note that we consider a perturbation along the y direction, which is approximately parallel to the long axis of the myosin (see Fig. 1). We have also studied the cases with perturbations

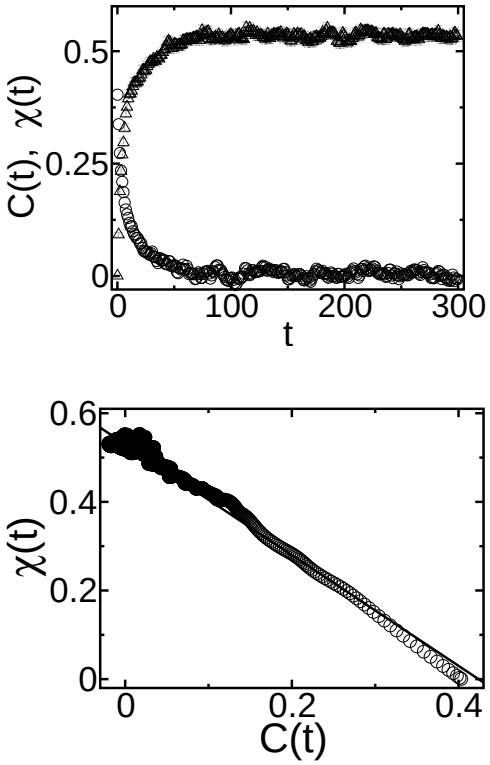

FIG. 2: (*Top*) $C(t)$ (circles) and $\chi(t)$ (triangles) plotted as functions of time in the equilibrium case with $T = 0.8$, $\Delta = 0.05$ and $k = 2\pi/10$. (*Bottom*) $\chi(t)$ as a function of $C(t)$ in the case $T = 0.8$. The slope of the line here is $-1/T$. In both graphs, the data points are obtained by averaging 2000 independent trajectories, and the statistical error bars are smaller than the symbols.

along different directions, and the results obtained in all cases are qualitatively the same as those obtained along the y direction. In this relaxation process, the susceptibility, $\chi(t)$, is defined as

$$\chi(t) \equiv -\frac{\langle \hat{\rho}(k,t) - \hat{\rho}(k,0) \rangle^{V_{\rm P}}}{\Delta}, \tag{8}$$

where $\langle\ \rangle^{V_{\rm P}}$ denotes the statistical average under this relaxation process. Writing the density in the y direction as $\rho(y,t) \equiv \sum_{i=1}^{N} \delta(y - y_i(t))/N$, we denote its Fourier transform by $\hat{\rho}(k,t)$:

$$\begin{aligned} \hat{\rho}(k,t) &\equiv \int_{-\infty}^{\infty} {\rm d}y \rho(y,t) \cos(ky) \\ &= \frac{1}{N} \sum_{i=1}^{N} \cos(k y_i(t)). \end{aligned} \tag{9}$$

Next, we define the density correlation function, which is computed in equilibrium without adding $V_{\rm P}$, as

$$C(t) \equiv \langle \hat{\rho}(k,t) \hat{\rho}(k,0) \rangle\, N. \tag{10}$$

Then, the following is one representation of the fluctuation-response relation:

$$R(t) = -\frac{1}{T} \frac{{\rm d}C(t)}{{\rm d}t}, \tag{11}$$

where $t \geq 0$ [10]. Here, the density response function, $R(t)$, defined as the time derivative of $\chi(t)$:

$$R(t) \equiv \frac{{\rm d}\chi(t)}{{\rm d}t}. \tag{12}$$

In numerical experiments, we computed $\chi(t)$ in order to investigate the behavior of $R(t)$.

In the upper graph of Fig. 2, $\chi(t)$ and $C(t)$ are plotted as functions of time with $T = 0.8$, $k = 2\pi/10$ and $\Delta = 0.05$. In the lower graph of Fig. 2, $\chi(t)$ is plotted as a function of $C(t)$. The fact that the slope of the lower graph is $-1/T$ indicates that the fluctuation-response relation (11) holds in equilibrium (the high temperature regime). Note that we set $k = 2\pi/10$ here because the lengths of the alpha helices in myosin are of the order of 10 Å. Glassy behavior of the density correlation and the density response is observed in the case $k = 2\pi/\ell$ with $\ell \geq 10$, as described below.

IV. NON-EQUILIBRIUM BEHAVIOR I: GLASSY PHENOMENON AT LOW TEMPERATURE

In this section, we consider simulations in which we quenched the system from $T = 0.5$ to $T = 0.05$ in order to investigate its glassy behavior. In this model, room temperature roughly corresponds to $T = 0.1$, which is estimated by comparing the mean square fluctuations of the C_α atoms in the model with those obtained in an all-atom model (data not shown). Therefore, the quenched temperature $T = 0.05$ roughly corresponds to 150 K, which is below the glass transition temperature of a real protein [18]. Note that myosin remains in a folded form even under conditions corresponding to $T = 0.5$.

In our simulations, we quench the system at $t = -t_{\rm w}$, and then we begin investigating the behavior of the system at $t = 0$. The quantity $t_{\rm w}$ is called the "waiting time." In general, relaxational glassy systems do not possess invariance with respect to time translation, and both correlations and responses decay more slowly as the age of the system increases. Thus, in such systems, correlation functions and response functions depend on $t_{\rm w}$.

In order to elucidate the glassy behavior of our system, we first introduce the auto-correlation function

$$F(t, t_{\rm w}) \equiv \left\langle \frac{1}{N} \sum_{i=1}^{N} [\cos(y_i(t) - y_i(0)) - \cos(y_i^0 - y_i(0))] \right\rangle_{t_{\rm w}}, \tag{13}$$

where $\langle\ \rangle_{t_{\rm w}}$ represents the statistical average under the relaxation we consider. (Auto-correlation functions are often employed in the study of glassy systems [4, 5, 6, 7,

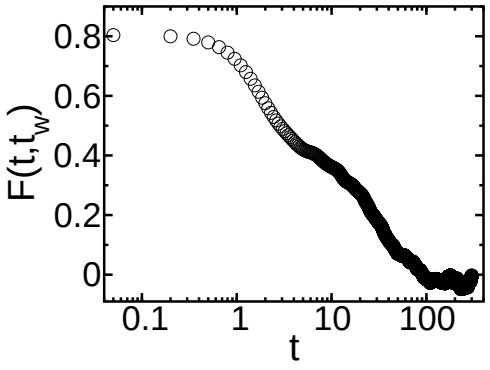

FIG. 3: $F(t, t_{\rm w})$ as a function of time for the case $t_{\rm w} = 100$. The data points are obtained by averaging 2000 independent trajectories, and the statistical error bars are smaller than the symbols.

8, 9].) The quantity $F(t, t_{\rm w})$ is a measure of the similarity of the configuration of the system at time t to that at time 0; note that the quantity $\cos(y_i(t) - y_i(0))$ is equal to 1 at $t = 0$ and decreases as t increases. The second term on the righthand side of (13) ensures that $F(t, t_{\rm w}) = 0$ for large t, because the configuration of the system, $\{\boldsymbol{r}_i(t)\}$, fluctuates about that of the native structure, $\{\boldsymbol{r}_i^0\}$, at large t. Computing $F(t, t_{\rm w})$, we canelucidate the slow relaxation of the configuration of the system. In Fig. 3, we plot $F(t, t_{\rm w})$ as a function of time for the case $t_{\rm w} = 100$. The form of the decay, which is not exponential, reveals the slow relaxation of the configuration.

V. NON-EQUILIBRIUM BEHAVIOR II: VIOLATION OF THE FLUCTUATION-RESPONSE RELATION AT LOW TEMPERATURE

In an aging system, the susceptibility, density response function and density correlation function, which depend on $t_{\rm w}$, are defined by

$$\chi(t, t_{\rm w}) \equiv -\frac{\langle \hat{\rho}(k,t) - \hat{\rho}(k,0) \rangle_{t_{\rm w}}^{V_{\rm P}}}{\Delta}, \tag{14}$$

$$R(t, t_{\rm w}) \equiv \frac{{\rm d}\chi(t, t_{\rm w})}{{\rm d}t}, \tag{15}$$

$$C(t, t_{\rm w}) \equiv \langle \hat{\rho}(k,t)\hat{\rho}(k,0) \rangle_{t_{\rm w}} N. \tag{16}$$

Note that $\langle\ \rangle_{t_{\rm w}}^{V_{\rm P}}$ denotes the statistical average under the condition that we quench the system at $t = -t_{\rm w}$, and switch on the perturbation potential given by (7) at $t = 0$. In the upper graph of Fig. 5, $C(t, t_{\rm w})$ and $\chi(t, t_{\rm w})$ are plotted as functions of time for the case $t_{\rm w} = 100$. The relaxations of $C(t, t_{\rm w})$ and $\chi(t, t_{\rm w})$ seem to be slow in comparison with those of $C(t)$ and $\chi(t)$ found in the equilibrium case with $T = 0.8$ (see the upper graph in Fig. 2).

In the lower graph of Fig. 4, we plot $\chi(t, t_{\rm w})$ as a function of $C(t, t_{\rm w})$ for the cases $t_{\rm w} = 100$ and $t_{\rm w} = 200$. It is seen that there are two slopes, characterizing two time regimes, unlike in the equilibrium case (see the lower graph in Fig. 2). The results plotted in Fig. 2 suggest that in the early regime, the form of $\chi(t, t_{\rm w})$ as a function of $C(t, t_{\rm w})$ approaches a line of the slop $-1/T$, where $T = 0.05$, as $t_{\rm w}$ increases. (See Fig. 16 of Ref. [9] for such observation of similar behavior.) In the late time regime, the form of this function is again a line, but in this case, the slope differs significantly from $-1/T$. (Also note that in this case, similar linear behavior is observed for both $t_{\rm w} = 100$ and $t_{\rm w} = 200$.) Such behavior of $\chi(t, t_{\rm w})$ and $C(t, t_{\rm w})$ is often observed in aging systems, including structure glasses [4, 5] and spin glasses [4, 6]. In an aging system, the slope of $\chi(t, t_{\rm w})$ as a function of $C(t, t_{\rm w})$ in the late regime is $-1/T_{\rm eff}$ where $T_{\rm eff}$ is called the effective temperature, and is defined through the relation

$$R(t, t_{\rm w}) = -\frac{1}{T_{\rm eff}} \frac{{\rm d}C(t, t_{\rm w})}{{\rm d}t}. \tag{17}$$

We interpret this behavior as indicating that in the early regime, the system relaxes toward the local equilibrium represented by a meta-stable state, while in the late regime, the system wanders among many meta-stable states, as it evolves toward the minimum of the free energy of the system. These two kinds of relaxational processes exhibited by an aging system are characterized by the two slopes $-1/T$ and $-1/T_{\rm eff}$.

The fact that $T_{\rm eff} \neq T$ represents a violation of the fluctuation-response relation in this aging system. The lack of invariance with respect to time translation and the violation of the fluctuation-response relation are a basic properties of relaxational glassy systems. The effective temperature $T_{\rm eff}$ denotes the difference of the system from equilibrium.

Before ending this section, we note an important point regarding $T_{\rm eff}$. The inequality $T_{\rm eff} > T$ is observed in many glassy systems [4, 5, 6, 7, 8, 9]. However, because there are counterexamples, the universality of this inequality has not yet been established. Here, we found $T_{\rm eff} > T$ in the elastic network model. Possible implications of this inequality in biological contexts are discussed below.

VI. $T_{\rm eff}$ FOR THE HEAD AND TAIL

One of the biggest differences between a structure glass and a protein is that a protein has characteristic substructures that are believed to cause a smoothing of the energy landscape, which makes the collective motion necessary for biological functions possible. As mentioned above, a myosin molecule is composed of a head, with ATP-binding and actin-interacting sites, and a tail, with a long alpha-helix bound by two light chains. It is interesting to compare these two parts with respect to $T_{\rm eff}$.

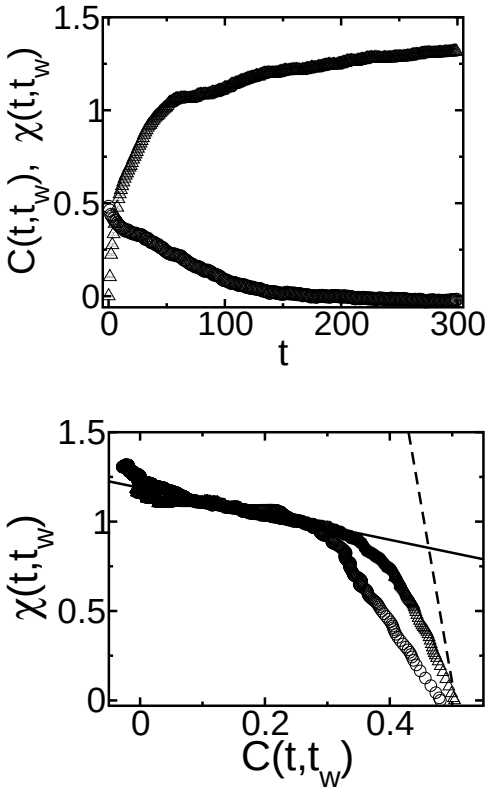

FIG. 4: (*Top*) $C(t,t_{\rm w})$ (circles) and $\chi(t,t_{\rm w})$ (triangles) plotted as functions of time in the case of an aging system, with $t_{\rm w} = 100$, and $\Delta = 0.05$ and $k = 2\pi/10$. (*Bottom*) $\chi(t,t_{\rm w})$ as a function of $C(t,t_{\rm w})$ for the cases $t_{\rm w} = 100$ (circles) and $t_{\rm w} = 200$ (triangles). The slope of the dotted line is $-1/T$, where $T = 0.05$. The slope of the solid line is $-1/T_{\rm eff}$, where $T_{\rm eff} = 1.3$. In both graphs, the data points are obtained by averaging 2000 independent trajectories, and the statistical error bars are smaller than the symbols.

For this purpose, we investigated the density response function and density correlation function for the head ($i = 1, \cdots, 770$) and the tail ($i = 771, \cdots, N$), and computed $T_{\rm eff}$ for each.

We define the Fourier transform of the density for the head and tail as

$$\hat{\rho}_{\rm h}(k,t) \equiv \frac{1}{770}\sum_{i=1}^{770}\cos(ky_i), \tag{18}$$

$$\hat{\rho}_{\rm t}(k,t) \equiv \frac{1}{N-770}\sum_{i=771}^{N}\cos(ky_i). \tag{19}$$

Then, we use $\hat{\rho}_{\rm h}(k,t)$ and $\hat{\rho}_{\rm t}(k,t)$ instead of $\hat{\rho}(k,t)$ in (14) and (16). Also, letting $N_{\rm h} = 770$ and $N_{\rm t} = N - 770$ be the total numbers of C_α atoms in the head and tail, respectively, we use these in place of N in (14) and (16). We note here that when computing the response functions, we add a perturbing potential of the form given in (7) only to the substructure under investigation.

In Fig. 5, we plot $\chi(t,t_{\rm w})$ as a function of $C(t,t_{\rm w})$ for both the head and the tail, respectively. We find that the effective temperature, $T_{\rm eff}$, for the head is higher than that for the tail. This implies that the structure of the head is more glassy than that of the tail.

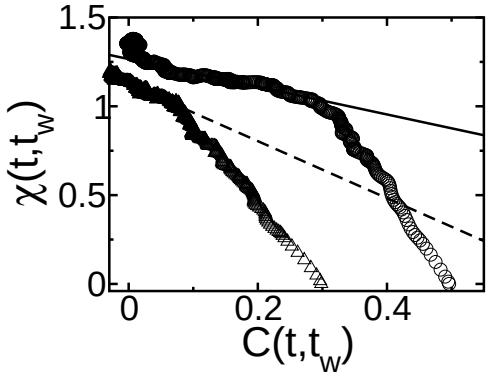

FIG. 5: $\chi(t,t_{\rm w})$ as a function of $C(t,t_{\rm w})$ in the case $t_{\rm w} = 100$ and $k = 2\pi/10$ for the head (circles) and the tail (triangles) of the myosin molecule. The slope of the solid line is equal to $-1/1.3$, while the slope of the dotted line is equal to $-1/0.6$. The data points are obtained by averaging 2000 independent trajectories, and the statistical error bars are smaller than the symbols.

VII. DISCUSSION

In conclusion, we investigated the glassy behavior of an elastic network model of the myosin molecule by studying the density correlation function and the density response function in the case that we quench the system from $T = 0.5$ to $T = 0.05$. The glassy behavior is displayed in Figs. 4 and 5, where the susceptibility, $\chi(t,t_{\rm w})$, is plotted as a function of the correlation function, $C(t,t_{\rm w})$. We found that $T_{\rm eff}$ defined in (17) was not equal to T, and thus that the fluctuation-response relation is violated. We also compare the degrees of the violation of the fluctuation-response relation for both the head and tail substructures of myosin, individually, and we found that $T_{\rm eff}$ is higher for the head than for the tail. In the following, we discuss two points related to these main results.

A. Effective temperature of the myosin molecule

Although further studies are required to ascertain physically clear interpretations of the effective temperature, the fact that $T_{\rm eff}$ is higher than T is intriguing, because it may be related to energy transduction taking place after ATP hydrolysis in a myosin molecule.

An acto-myosin system, of which a myosin molecule is a component, is a representative motor-protein system, and it has been studied in single-molecule experiments [19, 20, 21]. Upon binding of ATP to a myosin molecule, the myosin molecule detaches from an actin

filament. ATP hydrolysis takes place in the detached myosin molecule. The products of the ATP hydrolysis (ADP and an inorganic phosphate) are then released from the myosin molecule, which are thought to be coupled with the force exertion and with the re-attachment of myosin to the actin filament. Recently, a single-molecule experiment on an acto-myosin system demonstrated that the force exertion of the myosin molecule sometimes occurs *after* the release of the bound ADP [19]. This fact leads us to believe that the energy provided by the ATP hydrolysis might be stored in the myosin molecule for a short time before the force is exerted. If this is indeed the case, it is important to determine the form in which this energy is stored. The effective temperature, $T_{\rm eff}$, might help us solve this problem. Because ATP hydrolysis takes place only in the head, and because $T_{\rm eff}$ is higher in the head than in the tail, it is reasonable to conjecture that this energy storage has a close connection with the inequality $T_{\rm eff} > T$. To elucidate this connection is a future problem.

B. Inherent structures

Next, we discuss the origin of the glassy behavior observed in the elastic network model we study. In Fig. 6, we plot $E_{\rm IS}$, which is the total potential energy, $V + V_{\rm trap}$, when the system is at a local minimum in the energy landscape, as a function of time. The quantity $E_{\rm IS}$ is computed by using the steepest-descent energy-minimization method, as has been employed in Ref. [3], in the case $t_{\rm w} = 100$. From the rather discretized forms of the trajectories, it is seen that the system moves from one meta-stable state to another. We stress that the elastic network model described by (2) is not a harmonic system, and hence can possess local energy minima, although the model may appear to be a harmonic system (Actually, existense of local energy minima in an elastic network model is indicated in Ref. [22]).

It would be interesting to examine the difference between the native structure and the structures corresponding to the local energy minima (i.e., inherent structures). The upper graph of Fig. 7, displays the difference $|y_i^{\rm IS} - y_i^0|$ between the positions of the C_α atoms in the inherent structure and in the structure, 1KK7, where $\{y_i^{\rm IS}\}$ is the y value of the position of the i-th C_α atom in the inherent structure. From this graph, it is seen that the differences for some of the C_α atoms are as much as 10 Åand that those C_α which exhibit such large displacements are not localized but, rather, clustered.

Several structural isomers of myosin have been experimentally found by using X-ray crystallography [23]. The structure we studied here, 1KK7, is one with no nucleotide bound. Therefore, it would be interesting to compare the inherent structures with those of myosin isomers. As an example, we compare one of these inherent structures with the structure of the myosin isomer with an ATP-analog bound, 1KK8 [17]. The lower

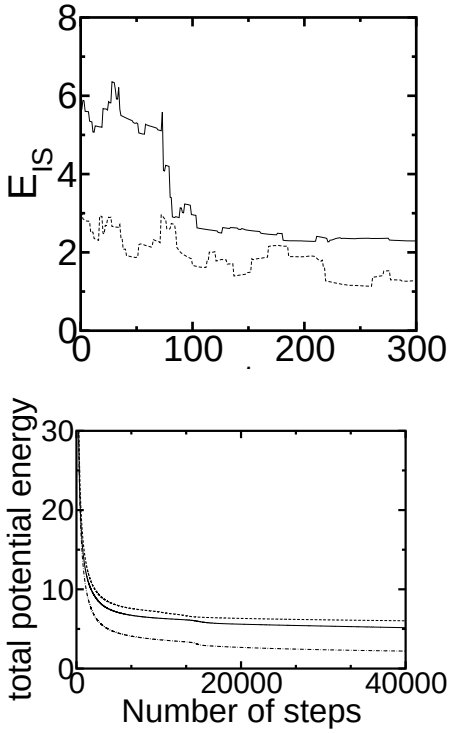

FIG. 6: (*Top*) Two examples of $E_{\rm IS}$, computed using the steepest-descent energy-minimization method, plotted as functions of time in the case $t_{\rm w} = 100$. (*Bottom*) Three examples of the steepest-descent energy-minimization trajectories are shown. Note that the three energy-minimization trajectories, with different initial configuratio ns (i.e., different "instantaneous structures" on the MD trajectory), tend to converge at different energy values.

graph in Fig. 7 shows that there is a resemblance between the inherent structure and the structure of the myosin isomer, with relatively large displacements seen near the N-terminal domain, the lower-50k domain, and the converter domain. This suggests that the elastic network model contain information concerning the structures of other isomers. Using a normal mode analysis for an elastic network model of a myosin molecule, Zhen and Doniach have shown that a structural isomer is located along the directions of some of the slowest modes of the structure [11]. Our results appear to be consistent with their results. Furthermore, our results indicate the meta-stability of the isomer. We believe that our results may lead to an extension of the applicability of the elastic network model of proteins, noting that it has been shown that this model can even be applied to the study of protein folding [24] and the investigation of nonlinear relaxation dynamics [22]. To elucidate the range of applicability of the elastic network model, we need to systematically study its meta-stable states for many kinds of proteins.

Acknowledgments

The authors acknowledge K. Komori for discussions concerning the experimental studies of acto-myosin systems and H. Takagi for facilitating these discussions. We also acknowledge M. Otsuki and K. Hukushima for discussions of glassy systems and A. S. Mikhailov and Y. Togashi for discussions of elastic network models. This work was supported by grants from JSPS Research Fellowships for Young Scientists and the Ministry of Education, Science, Support and Culture of Japan.

[*] Electronic address: hayashi@jiro.c.u-tokyo.ac.jp, mtkn@waseda.jp

[1] Frauenfelder, H., Wolynes, P. G. and Austin, R. H. (1999) *Rev. Mod. Phys.* **71** S419-S430.
[2] Nakagawa, N. and Payrard, M. (2006) *Proc. Natl. Acad. Sci. USA* **103**, 5279-5284.
[3] Stillinger, F. H. and Weber, T. A. (1982) *Phys. Rev. A* **25**, 978-989.
[4] Crisanti, A. and Ritort, F. (2003) *J. Phys. A* **36**, R181-R290.
[5] Berthier, L. and Barrat, J-L. (2002) *Phys. Rev. Lett.* **89**, 095702.
[6] Cugliandolo, L. F., Kurchan, J., and Peliti, L. (1997) *Phys. Lev. E* **55**, 3898-3914.
[7] Ono, I. K., O'Hern, C. S., Durian, D. J., Langer, S. A., Liu, A. J. and Nagel, S. R. (2002) *Phys. Rev. Lett.* **89**, 095703.
[8] Kolton, A. B., Exartier, R.,Culiangolo, L. F., Domíguez, D. and Grønbech-Jensen, N. (2002) *Phys. Rev. Lett.* **89**, 095703.
[9] Cugliandolo, L. F. (2002) *e-print* cond-mat/0210312.
[10] Hayashi, K., and Sasa, S. (2006) *Physica A* **370**, 407-429.
[11] Zheng, W. and Doniach, S. (2003) *Proc. Natl. Acad. Sci. USA* **100**, 13253-135258.
[12] Navizet, I., Lavery, R. and Jernigan, R. L. (2004) *Proteins* **54**, 384-393.
[13] Tirion, M. M. (1996) *Phys. Rev. Lett.* **77**, 1905-1908.
[14] Atilgan, A. R., Durell, S. R., Jernigan, R. L., Demirel, M. C., Keskin, O. and Bahar, I. (2001) *Biophys. J.* **80**, 505-515.
[15] Takano, M., Higo, J., Nakamura, H. K. and Sasai, M. (2004) *Nat. Comput.* **3**, 377-393.
[16] RCSB PROTEIN DATA BANK, http://www.rcsb.org/pdb/Welcome.do.
[17] Himmel, D.M., Gourinath, S., Reshetnikova, L., Shen, Y., Szent-Gyorgyi, A.G. and Cohen, C. (2002) *Proc. Natl. Acad. Sci. USA*. **99**, 12645-12650.
[18] Austin, R. H., Einstein, L., Frauenfelder, H. and Gunsalus, I. C. (1975) *Biochemistry* **14**, 5355-5373.
[19] Ishijima, A., Kojima, H., Funatsu, T., Tokunaga, M., Higuchi, H., Tanaka, H. and Yanagida, T. (1998) *Cell* **92**, 161-171.
[20] Kitamura, K., Tokunaga, M., Iwane, A. H. and Yanagida, T. (1999) *Nature* **397**, 129-134.
[21] Iwaki, M., Tanaka, H., Iwane, A. H., Katayama, E., Ikebe, M. and Yanagida, T. (2006) *Biophys. J.* **90**, 3643-3652.
[22] Togashi, Y. and Mikhailov., A. S. (2007) *Proc. Natl. Acad. Sci. USA*. **104**, 8697-8702.
[23] Houdusse, A. and Sweeney, H. L. (2001) *Curr. Opin. Struct. Biol.* **11**, 182-194.
[24] Micheletti, C., Lattanzi, G. and Maritan, A. (2002) *J. Mol. Biol.* **321**, 909-921.

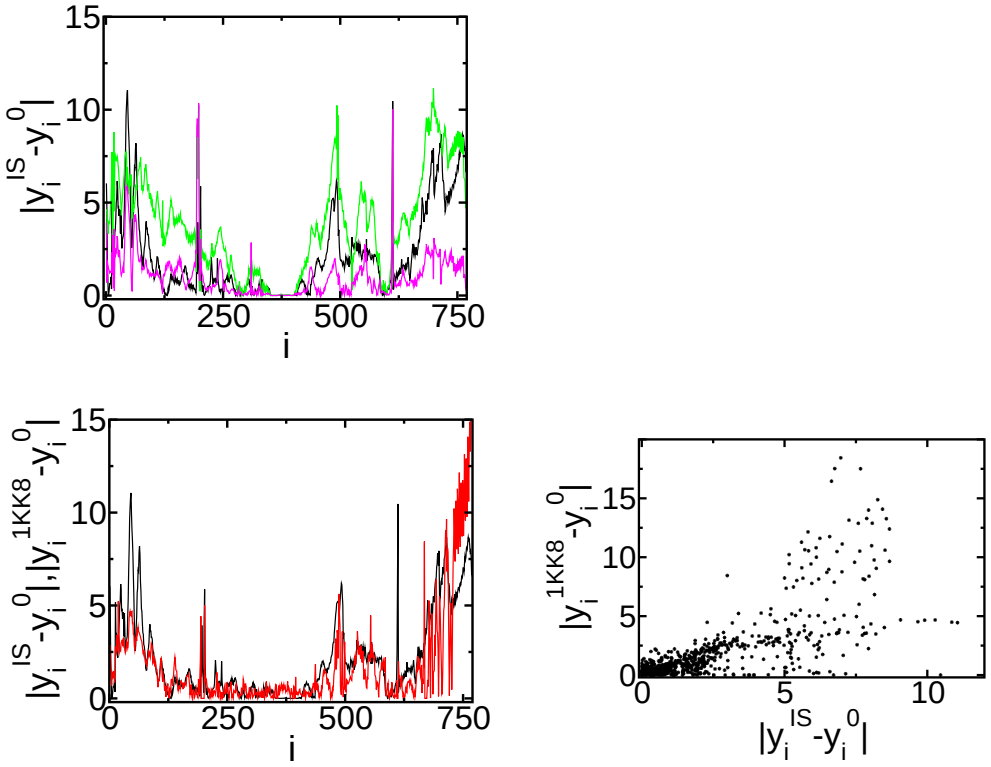

FIG. 7: (*Top*) Three examples (black, pink, green) of $|y_i^{\rm IS} - y_i^0|$ plotted as functions of i ($1 \le i \le 770$, the head substructure in our definition), where $\{y_i^{\rm IS}\}$ is a configuration computed using the steepest-descent energy-minimization method, and $\{y_i^0\}$ is the configuration of the structure 1KK7. Note that the α-carbon atoms, C_α, with $i = 350, \cdots, 400$ are trapped by $V_{\rm trap}$ (see (3)). (*Bottom, Left*) An example of $|y_i^{\rm IS} - y_i^0|$ (black) and $|y_i^{\rm 1KK8} - y_i^0|$ (red) plotted as functions of i. Here, $\{y_i^{\rm 1KK8}\}$ is the configuration of the structure 1KK8. (*Bottom, Right*) $|y_i^{\rm 1KK8} - y_i^0|$ plotted as a function of $|y_i^{\rm IS} - y_i^0|$.